

## PRESSURE TUBE BALLOONING EXPERIMENTS ANALYSIS

Jovica R. Riznic and Lorne D. Macdonald  
Atomic Energy Control Board  
Safety Evaluation Division "Analysis"  
Ottawa, Ontario K1P 5S9

### ABSTRACT

Integrity of pressure tubes is one of the milestones in achieving safe operation of nuclear power plants with CANDU reactors. The aim of a safety analysis is to demonstrate pressure tube integrity by showing that the pressure tube does not rupture both: (1) when it balloons (because of local strain), and (2) after it contacts the calandria tube. Therefore, the ability to model pressure-tube ballooning is a key step in the licensing analysis of a CANDU reactor during a postulated loss-of-coolant accident.

AECB sponsored an experimental research project at the Stern Laboratory [1] to address the repeatability of pressure tube ballooning data and to demonstrate the effect of bearing pad fretting on rupture. This research project is part of a broader study on the effect of in-service degradation on the ballooning behaviour of pressure tubes. Newly performed experiments, in the Phase 5 of the research project [2], comprised the testing of nine pressure tube specimens to study the effects of hydride blisters and uniformly distributed hydrogen, and the composition of the internal pressurizing gas, including argon, steam, a steam-iodine mixture and hydrogen. A phase to test irradiated tubes has been put on hold pending results of COG tests.

As a part of continuing support of the research project on pressure tube ballooning, the present work concentrated on resimulation of the newly performed experiments by using three computer codes, e.g., PTDFORM, PTSTRAIN and AECBALL. Intercode comparisons show that code calculated results for strain rates and time of failure are close to each other, for nonuniform ballooning under specified conditions. However, it can be seen that both codes largely under predict the creep rate and experimental failure strains. The factor, among others, that may be contributing significantly to the poor agreement between the codes is clearly nonlinear character of the straining. One of the sources of nonlinearity may certainly be attributed to the localized irreversible heat generation due to the deformation work done on the pressure tube, particularly around the location of the failure. This effect is not considered in either one of the codes used for pressure tube integrity analysis. Obviously, ballooning and straining in the plastic deformation region cannot be easily addressed with simple mechanistic models used in these codes.

### INTRODUCTION

After years of development, the existing nuclear safety codes are today already used over a wide range of applications such as: licensing, accident analysis, optimization of plant procedures and setpoints and even support of design changes. Although each of these activities could be afforded with scenario and plant specific models and codes, in practice it is quite common to use a single model or single code for as many scenarios and applications as possible. This increases the complexity and uncertainties besides those inherent to the codes themselves. Validation of the capabilities of any of those codes are dealt by comparing the code predictions with the measured data obtained from various types of separate effects and integral test facilities. The amount of validation evidence required case by case depends upon a number of factors, such as: the complexity of the phenomena involved, importance in relation to safety issues or quality of information supplied in support of analysis. AECB requires a systematic approach to code validation in order to clearly identify those applications for which any particular code is adequately validated.

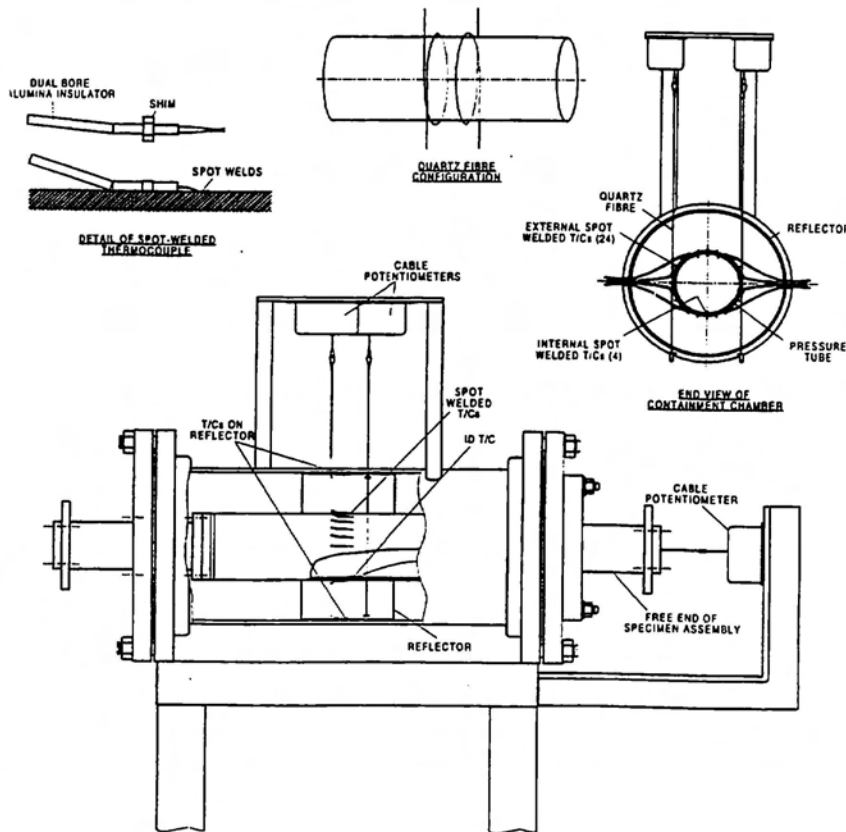
Pressure tubes represent the second safety barrier, which separate the fuel and coolant from the heavy-water neutron moderator. Under normal operating conditions pressure tubes are exposed to the temperatures in the range of 250 to 310°C and to internal pressure of more than 10 MPa. The safety story commonly assumed by the licensees is based upon a postulated loss-of-coolant accident causing degradation of coolant flow which may become stagnant or stratified in some of fuel channels. The coolant inside pressure tubes may boil off, causing a portion of the fuel bundle and

pressure tube to become exposed to superheated steam as the coolant level in the channel drops. Such a sequence of the events would result in a circumferential temperature gradient around the pressure tube. The resulting circumferential temperature gradient with high internal pressure would induce localized stresses and nonuniform deformation (ballooning) of the pressure tube. Integrity of pressure tubes is one of the milestones in achieving safe operation of nuclear power plants with CANDU reactors. The licensees demonstrate pressure tube integrity by showing that the pressure tube does not rupture both: (1) when it balloons (because of local strain), and (2) after it contacts the calandria tube. Therefore, the ability to model pressure-tube ballooning is a key step in the safety analysis of a CANDU reactor during a postulated loss-of-coolant accident.

#### AECB EXPERIMENTAL PROGRAM ON PRESSURE TUBE BALLOONING

AECB launched an experimental research project at the Stern Laboratory to address some aspects of the pressure tube ballooning and to gather new experimental data to validate computer codes used in safety analysis. This research project is part of a broader study on the effect of in-service degradation on the ballooning behaviour of pressure tubes. The test section consists of a 450 mm long section of Zr-2.5 wt% Nb CANDU pressure tube specimen supported inside a containment chamber. Electrical bus-bars from a 156 kVA, single phase, alternating current power supply and transformer were attached to extensions on each side of the specimen. The pressure tube specimen is directly resistance heated to provide a temperature ramp rate of up to about 35 Ks<sup>-1</sup>. The inside of the specimen is pressurized with steam from an electrically heated pressurizer or with other gases (argon, hydrogen or iodine) from regulated cylinders. An argon/CO<sub>2</sub> purge is maintained outside the specimen. Test section and instrumentation schematic is shown in Figure 1.

**Figure 1**  
**Test Section and Instrumentation Schematic [2]**



The specimens for tests were fabricated from two as-fabricated Zr-2.5 wt% Nb CANDU pressure tubes, manufactured by Nu-Tech Precision Metals Inc. Specimen Numbers 8, 9, 10 and 11 were cut from a tube BB161 which was manufactured using a quadruple-melted ingot material and the current standard fabrication schedule for CANDU Zr-2.5%Nb pressure tubes. Specimen Numbers 1 through 5 were cut from a tube TG098MC which was manufactured using a double-melted ingot material and the Task Group Three - Route 1 (TG3-R1) fabrication schedule. The specimens are 450 mm long with titanium end caps attached with full penetration welds. Specimen Numbers 8, 9 and 10 were treated for hydriding and blistering in the Ontario Hydro Technology laboratories. The treatments consisted of electrolytically hydriding the tubes to the desired hydrogen concentration and then growing blisters using the air jet technique. This involves heating the inside surface of the tube using liquid metal and locally cooling the outer surface with a jet of air to generate the blister.

The pressure tube temperature was measured with 24 chromel-alumel thermocouples spot-welded to the outside of the tube and four thermocouples on the inside surface. The internal pressure was controlled during the test and measured with a capacitance-type transmitter and a fast response strain gauge transducer. The pressure tube strain was measured with two quartz fibres which were wrapped around the tube at axial locations 30 mm on either side of the mid-plane. Electrical measurements include voltage, current and power on the high voltage side of the transformer, and voltage drop across the specimen. In all tests the pressure tube was free to balloon until it ruptured or the test was terminated when a specimen approached average circumferential strain of above 30%. The data from instrumentation were acquired, processed and stored on a DEC data acquisition system. The sampling rate was 20 Hz per channel. A detailed description of the experimental program, tests and experimental data for both series Phases 4 and 5, of experiments can be found in references [1] and [2], respectively.

## COMPUTER SIMULATION OF EXPERIMENTS

The simulations of the recent-Phase 5 experiments of the experimental program on pressure tube ballooning were performed with the three different computer codes. Namely, we have used the PTDFORM, the PTSTRAIN and the AECBALL computer codes. Simulations were done with the licensee codes for two reasons: The reference tests were not at exactly the same conditions as the tests with degraded tubes so simulations were used to account for such differences. Also, the simulations are to confirm that the codes are valid for the reference tests.

PTDFORM(Pressure Tube DeFORMATION) is a computer code developed at AECL using membrane theory to calculate pressure tube ballooning within the calandria tube during postulated LOCA conditions. Heat transfer to or from the pressure tube is not modelled in PTDFORM. The code uses input temperature and pressure transients to determine the strain of the pressure tube. The strain calculation is based on the creep rate correlation developed by Shewfelt from uniaxial creep tests on specimens of Zr-2.5wt% Nb tubes [3, 4].

One of the basic assumptions made in code development is that the pressure tube cross section remains circular as the tube strains, while the wall thickness strains non-uniformly. The present, Version 2.0 of the code is documented in References [5, 6]. Unfortunately, only half (180 degrees) of a pressure tube can be modelled at a time by this computer code. Therefore, experimental data for input temperature and wall thickness profiles had to be split into two parts.

A symmetric temperature distribution is assumed for the other half. The tube is divided into a user specified number of azimuthal nodes (segments). The maximum number of nodes is 180, allowing up to one node per degree around the circumference. Using the input pressure and temperature profiles and a Zr-2.5 wt % Nb creep correlation, a strain rate is calculated for each node. The strain rate is used to determine a new node length and wall thickness. Summing the node lengths gives a new circumference and thus the average strains of the tube. For each link of the semicircular pressure tube approximation, the temperature, pressure, wall thickness and average tube radius are used to estimate the time step  $\Delta t$ . This time step should produce a maximum local strain increment no greater than the user selected input constant  $\Delta \epsilon$  (DEPSILN). At every time step, the local strain is calculated using the Euler method, and iterated until the convergence criterion based on the local strain and the fractional minimum wall thickness is satisfied at every radial node.

PTSTRAIN is a computer code, or rather a driver developed by Ontario Hydro. The PTSTRAIN [7] code uses a modified version of the NUBALL [8] routine from the SMARTT computer code [9]. The NUBALL routine was

modified to permit the modelling of defects on the pressure tube. PTSTRAIN models one half of the pressure tube with symmetry across the vertical diameter of the tube. The pressure tube is divided into a number of equal circumferential nodes, each node is assumed to be at a uniform temperature. For these simulations, with the code that we have been given by Ontario Hydro [10], the one half of the pressure tube was divided into 226 nodes. At each computational time step the transverse strain for each node is calculated and a new pressure tube circumference is determined. The radius of the pressure tube at the end of the time step is calculated from the new circumference and the new wall thickness is calculated with the assumption of constant pressure tube density (and element volume). In this procedure it is assumed that the pressure tube remains circular during the deformation. The computational step is controlled by the rate of transverse strain so that the true strain does not exceed  $10^{-3}$  per time step. Pressure tube failure is assumed to occur if the local radial strain exceeds 100 percent true strain, i.e., if the local wall thickness is reduced to 37 percent of its initial value.

The AECBALL code was developed by CQAD AECB [11, 12] to model the pressure tube as a whole tube cross section, without assuming symmetry about the vertical axis. The code assumes simple one-dimensional structural behaviour. The program can model flaws by using different wall thicknesses but does not include the effects of stress concentration. A failure criterion is based on the assumption that failure occurs when any element in the pressure tube model reaches 100% true strain. The code uses a creep relationship proposed by Shewfelt et al., [3, 4]. Also, the AECBALL code has an option of using "best fit" coefficients in the Shewfelt model for a creep rate, based on the data from Phase 4 of the AECB/Stern experimental program [1].

A common feature of these three codes is that all of them are based on the same mechanistic model of straining and use the same relationship for a creep rate. The transverse creep equation for as-received Zr-2.5% Nb pressure tubes, in the temperature range from 450 to 850°C, as proposed by Shewfelt et al., [3] is given by

$$\dot{\epsilon}_t = 1.3 \times 10^{-5} \sigma_t^9 e^{-\frac{36600}{T}} + \frac{5.7 \times 10^7 \sigma_t^{1.8} e^{-\frac{29200}{T}}}{\left[ 1 + 2 \times 10^{10} \int_{t_1}^t e^{-\frac{29200}{T}} dt \right]^{0.42}}$$

where  $\dot{\epsilon}_t$  is the transverse creep rate in  $s^{-1}$ ,  $\sigma_t = (p-p_0)r/w$  is the transverse stress in MPa,  $p$ - pressure inside the pressure tube (PT),  $p_0$ -pressure outside the pressure tube,  $w$ - thickness of PT,  $r$ - inner radius of PT,  $t$  is the time in s, and  $t_1$  is the time when  $T=973$  K. The first term describes the creep rate at temperatures below about 600 OC, and for stresses above about 200 MPa. At temperatures above 600°C, there is a change in the creep mechanism in Zr-2.5% Nb, which reduces the creep strength, and Zr-2.5% Nb becomes superplastic. The second term in the creep equation describes the creep rate in this superplastic region.

The transverse creep equation for as-received Zr-2.5% Nb pressure tubes in the temperature range 850 to 1200°C is [3],

$$\dot{\epsilon}_t = 10.4 \sigma_t^{3.4} e^{-\frac{19600}{T}} + \frac{3.5 \times 10^4 \sigma_t^{1.4} e^{-\frac{19600}{T}}}{1 + 274 \int_{t_2}^t e^{-\frac{19600}{T}} (T-1105)^{3.72} dt}$$

where  $t_2$  is the time when  $T=1123$  K. The first term describes the power law creep in the  $\beta$  phase, and the second term describes the grain- boundary sliding component. The grain-boundary sliding component is significant at temperatures between 850 and 950°C, when the  $\alpha$  phase to  $\beta$  phase transformation is rapid.

These transverse creep equations were developed using data from uniaxial creep tests in which the temperature and stress were held constant; in which the temperature was held constant and the stress was varied in steps to determine the stress exponent; and in which the stress was held constant and temperature was varied in steps to determine the activation energy [3]. These transverse creep equations were then verified using transient uniaxial and biaxial tests [4]. For the transient uniaxial tests, stresses from 5 to 130 MPa and temperature ramp rates from 1 to 50°Cs<sup>-1</sup> were used. For the transient biaxial tests, internal pressures from 0.5 to 10 MPa were used, and the temperature ramp was about 5°Cs<sup>-1</sup> below about 500°C and it dropped to about 1°Cs<sup>-1</sup> above 800°C. If a pressure tube balloons uniformly, it will come into full contact with its calandria tube at a transverse creep strain of about 18%. Consequently, the creep equations were used to predict the pressure tube temperature at which the transverse creep strain would be 18% (contact temperature) in the verification tests, and this was compared to the measured contact temperature. For contact temperatures below 850°C, the maximum difference in the measured and predicted contact temperatures was 35°C [4]. This illustrates that for the limited (as received Zr-2.5 % Nb) material used in the verification tests, the creep equations predicted the contact temperature fairly well. However, there is not sufficient creep data to accurately determine the creep rate distribution for irradiated the Zr-2.5% Nb pressure tubes now in CANDU reactors [13]. The possible effects of both irradiation damage, deuterium, hydrogen gas and iodine [14, 15] on the creep rate were not taken into account in the creep rate equations and in the ballooning model, and there is no reliable data to show that these would not affect the ballooning of pressure tubes.

Recently, Clark [16] used FLOTRAN, a computational fluid dynamics package included in the ANSYS FEM computer code, to simulate the Stern experimental tests. The analysis involved both, static and transient simulations. Heat was applied to the pressure tube model to develop the 35 Ks<sup>-1</sup> temperature ramp achieved in the experiments. Natural convection was modelled between the outside of the pressure tube and the inside of the containment chamber. The temperature profile around the pressure tube circumference obtained from the Flotran analysis was compared to the experimental data from the first series of tests at the Stern Laboratory. It reproduced the temperature gradient on the pressure tube, which changed more at the top than the bottom, but FLOTRAN was not able to interpret the asymmetry about the vertical axis. Temperature profiles from the Flotran analysis were used as an input to AECBALL to perform pressure tube creep analysis. A previous report by G. De Carufel [17], describes the simulation of the first set of experiments (Phase 4), performed in the Stern Lab [1]. Simulations of experimental results were done by using the computer code PTDFORM. Analyses of all 6 experiments showed that the PTDFORM code could not predict rupture if the raw experimental data was used. It was for this reason that the FLOTRAN analysis was done to have more information about the temperature gradient and more thermocouples were used at the top of the specimens in Phase 5 of the experimental program. Further, some discrepancies existed between the results for the two halves of the same tube and the experimental results.

As a part of continuing support of the research project on pressure tube ballooning, we resimulated the CQAD analyses [16] by using PTDFORM and AECBALL3 computer codes [18, 19]. Resimulation of the FLOTRAN analysis showed that PTDFORM and AECBALL3 largely under predict the creep rate and experimentally obtained data on failure strain. The present study is a continuation of the work on the pressure tube ballooning problem using new experimental data and another industry developed computer code. Running three different codes for each of nine experiments from the Phase 5 of AECB/Stern Lab experiments is a complex task with several pitfalls confronting the code analyst. Within the frame of the large international effort on the assessment of computer codes used for safety analysis of nuclear reactors, there has been a continuous debate on the way how the code analyst (code user) influences the predicted system behaviour. This rather subjective element might become a crucial point with respect to the quantitative evaluation of the code predictions and its accuracy. Pitfalls that can influence the code-calculated results exist primarily because of modelling approximations and deficiencies inherent to code themselves [20]. Due to the large number of files involved in simulation runs, management of these files presented a challenge for quality data analysis. A log file was thus established to keep track of these files and other files generated during data. It is also important to note that three codes used in these exercises were actually written for three different computer systems, e.g., PTDFORM was run on a HP715, PTSTRAIN on an IBM375 workstation and AECBALL on a PC. This was just another fact to add to the overall complexity of simulation exercises. In the process of the simulation exercise we try to follow some good modelling practice to minimize the occurrence of possible pitfalls. In all exercises the code developers recommended practice and options were used, including standard nodalization of the pressure tube, the computational time step control and temperature profile interpolation among other parameters. Experimental data were used as measured, and minor corrections were done only for physically unrealistic values which were an artifact of the measurement technique and not a physical phenomena. Temperature profiles for input decks for all three computer codes were prepared by an in-house

developed routine using the same measurement data set for every single experiment. Temperature profiles used in the present simulations were prepared using the data acquired by thermocouples located around the outside diameter of the specimen, without any correction for the usually lower temperature measured inside. Also, a certain number of sensitivity studies to check the integrity of the main calculations were performed. In addition, a limited number of hand calculations to check creep rates were performed during this study.

## SIMULATION RESULTS

A summary of test conditions and results for all nine tests from the Phase 5 of the experimental program on pressure tube ballooning is shown on Table 1. Rupture was taken as the time when the axial strain suddenly changed from positive to negative.

**Table 1**  
**Summary of Test Conditions and Results**

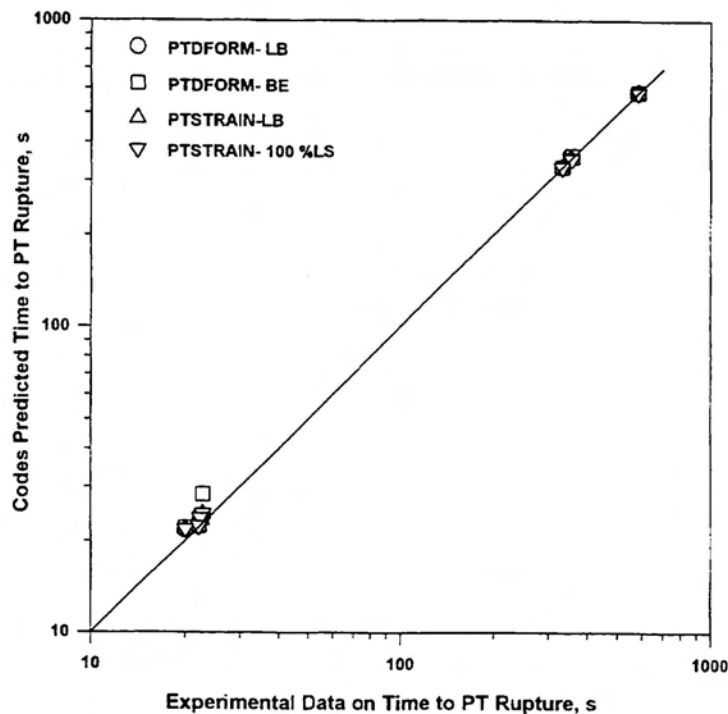
Test No.	A	B	C	D	F	G	E	H	I
Data Point	273	279	282	284	286	287	292	304	317
Test Objective	Ref. for D&F	Ref. for C	Iodine Effect*	H.Blisters ***	H.Blisters	H.Blisters	Hydrogen	Iodine	Ref. for G
Pressure, MPa (a)	6	6	6	6	6	9.6	1	1	9.6
Ramp rate, Ks <sup>-1</sup>	35	1	1	35	35	35	1**	1**	35
Time to Rupture, s	22.8	353	357	22.6	22.4	22.15	583 <sup>+</sup>	332 <sup>+</sup>	20.1
Location of Rupture, °	-10	-10	0	-10	-10	0	No Rupture	No Rupture	-10
Max. Top Temp. °C	770	712	711	786	781	723	827	864	727
Max. Bottom Temp. °C	738	642	639	754	753	691	794	842	692
Rupt. Cir. Strain@ -30mm, %	22.0	20.6	16.2	27.6	23.8	11.1	30.7 <sup>+</sup>	33.0 <sup>+</sup>	10.5
Rupt. Cir. Strain@ +30mm, %	20.0	29.8	26.1	27.3	25.4	10.0	38.4 <sup>+</sup>	34.9 <sup>+</sup>	9.1
Max. Circ. Str. Post Test, %	30.3	36.9	27.6	34.0	28.4	13.5	67.4	35.4	19.4
Loc of Max Str. mm	-60	0	0	0	0	-60	0	0	-90

Notes:

- \* - Actually only trace of Iodine was present in this case, due to a faulty delivery system
- \*\* - The rate increased from  $1\text{Ks}^{-1}$
- \*\*\* - Depth of Blisters for Experiment D was 0.15 mm and 0.7 mm for Experiments F and G
- + - End of temperature ramp for tests without rupture

A summary plot with comparison of the codes' predictions of the time of pressure tube rupture against data, for Phase 5 of the experimental program, is presented in Figure 2. Excellent agreement between the simulation results and experimentally obtained data is clearly shown. The predicted values of the time to rupture are within a few percent of the observed data, in most of the cases. However, a general trend can be noticed in the results with respect to the codes calculated results: the time to rupture is slightly under predicted. To permit the codes to predict the specimen rupture, it was necessary to let the codes to run for a longer period of time, by keeping both the temperatures and the pressure at their latest value (just prior to rupture) for additional time. For experiments with a high temperature ramp of  $35\text{Ks}^{-1}$ , this change in the input data resulted in rupture with delay ranging from about 0.25 to 1.5 seconds. This means the rupture/contact temperature can be predicted to within the interval of 10 to  $45^\circ\text{C}$ . More details on comparison between the codes' predictions and data can be seen in Table 2 for experiments on the effect of hydrogen blisters. For this particular set of experiments, there is also a scatter among the codes' results regarding location of pressure tube failure. However, for most of the experiments, the codes' predictions of the specimen rupture location agreed reasonably well with actual rupture location, as observed in experiment.

**Figure 2**  
**Comparison of Codes Prediction of Time to Rupture against Experimental Data**



For the reference case (A), PTDFORM does not predict the circumferential strain at rupture as well as PTSTRAIN, which is within 2%. PTSTRAIN reproduces test D within 1% so its shallow blisters (0.15 mm deep) and 40 ppm hydrogen have no effect on rupture strain. However, for test F, PTSTRAIN must use the lower bound rupture criteria to reproduce the experimental results so there may have been a small effect of 0.7 mm deep blisters and 150 ppm hydrogen content. This is unlikely since the rupture occurred  $10^\circ$  away from the blisters although the strain around each blister was certainly greater than the parent material's as shown in reference [21]. A similar argument shows that, although the code

results equal the experimental data for the blistered tubes at 9.6 MPa (Test G), the codes over predict the reference test at 9.6 MPa (Test I). So, although the circumference at rupture was the same with and without blisters, the codes do not expect them to be. Therefore, it appears that blisters had an effect of increasing the rupture strain at 9.6 MPa, but since the reference test (I) had a region with strain comparable to the code results 90 mm from its mid plane, the interpretation could be that the blisters had no effect. Byrne [22] performed set of calculations to investigate the status of hydride blisters during various temperature ramps up to 800°C. Calculations showed that for high temperature ramp 35 Ks<sup>-1</sup>, the blisters won't dissolve. The present experiments confirmed qualitative agreement with these calculations. Further investigation based on references [21, 22] and the present experiment could probably give more data for quantitative agreement and characterization of blisters.

**Table 2**  
**Summary Comparison of Test Results and Codes Prediction**  
**for the Experiments on the Effect of Hydrogen Blisters**

Parameter	Experiment*	PTDFORM Calculations **, ***		PTSTRAIN Calculations **, ***	
		LB	BE	LB	100% LS
	<b>A-273</b>				
Time to Rupture, s	22.8	24.1/NA	24.3/NA	24.4/25.8	24.6/26.0
Location of Rupture, °	-10	-22/No Rupture	-22/NA	-6.8/6.8	-6.8/6.8
Cir.Strain %	22.0/20.0	28.4/NA	35.1/NA	18.5/29.1	20.3/33.4
	<b>D-284</b>				
Time to Rupture, s	22.6	23.6/23.7	23.8/23.9	23.4/23.6	23.4/23.7
Location of Rupture, °	-10	-3/0	-3/0	-6.8/0	-6.8/0
Cir.Strain %	27.6/27.3	24.1/24.5	29.8/29.8	23.6/24.8	26.8/27.5
	<b>F-286</b>				
Time to Rupture, s	22.4	23.5/23.8	23.7/NA	23.7/23.8	23.8/23.9
Location of Rupture, °	-10	-10/0	-11/NA	-6.8/0.4	-6.8/0.4
Cir.Strain %	23.8/25.4	30.5/24.1	38.8/NA	25.4/23.3	29.3/25.3

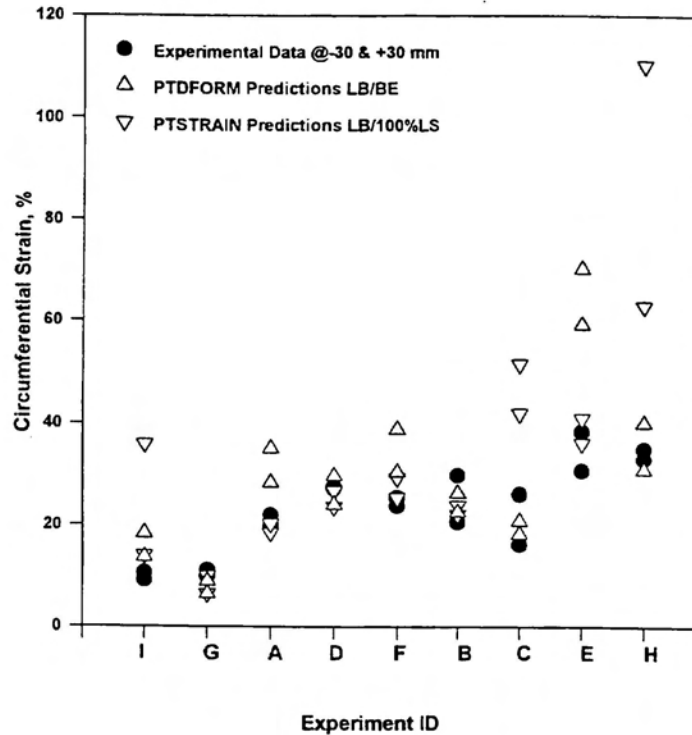
**Legend:**

- \* -Circ. Strain as measured @ -30mm /+30 mm from middle plane
- \*\* -Calculated values for left half/right half of the pressure tube
- \*\*\* -Minus sign for the location of rupture indicates the left half of the pressure tube, measured from the top
- LB; BE & 100% LS -Lower Bound; Best Estimate&100 % Local Strain Failure Criteria, respectively.

The simulation results in respect to average circumferential strain at the time of tube rupture are summarized in Figure 3. For the codes' predictions, the values of average strain for both, lower bound and best estimate or 100% local strain

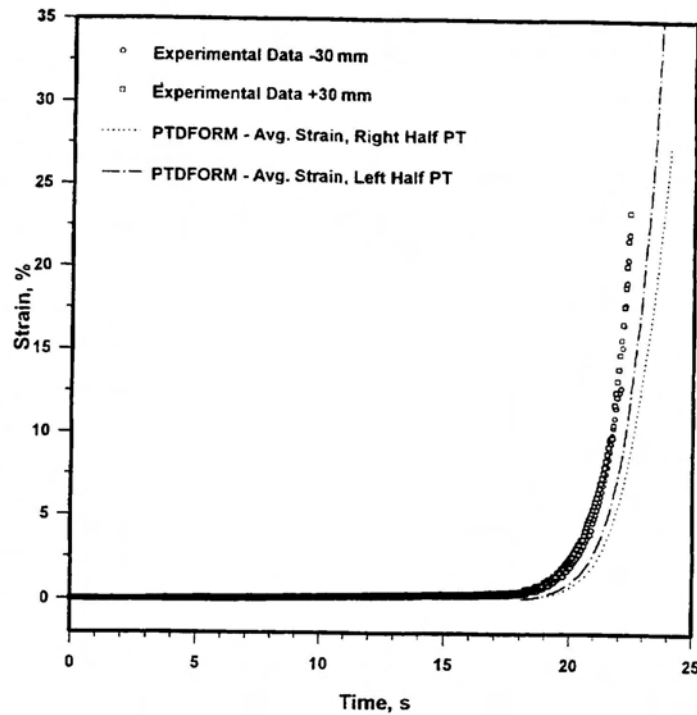
failure criteria are given in comparison with experimental data obtained by quartz fibres at -30 mm and +30 mm from the middle plane. In contrast to the results of time to failure, the average strain results show large scatters among the data. It should be noted here that in some of the experiments, the pressure tube continued to strain for a short period of time after rupture occurs or after termination of the experiment. This was caused because the pressure inside the tube did not fall to the atmospheric value immediately. This is the reason for discrepancies between the strain at the failure as measured by quartz fibres and the post test measurements of the strain around the specimen.

**Figure 3**  
**Comparisons of Codes Prediction of Average Circumferential Strain at the Time of Rupture**



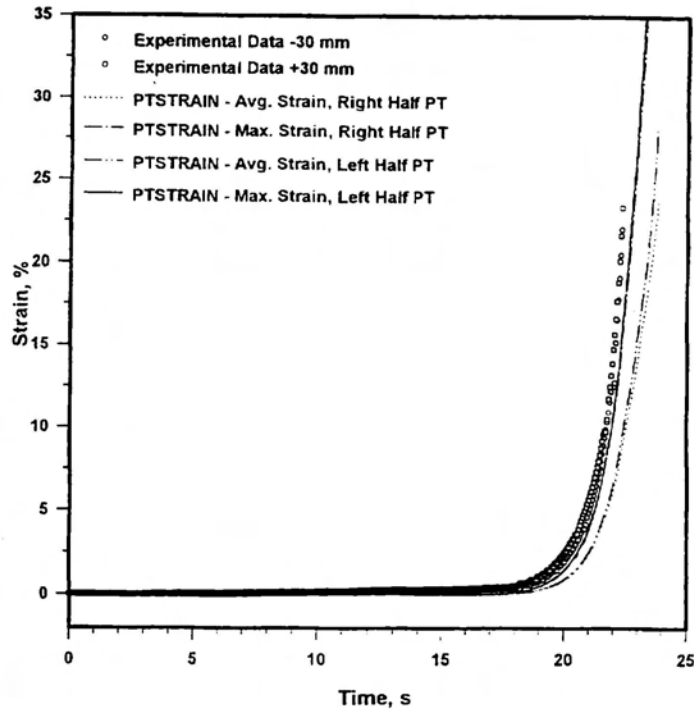
Intercode comparisons show that PTDFORM and PTSTRAIN results for strain rates and time of failure are close to each other, in most of cases analysed in these exercises. The overall agreement of the codes' predictions was rather qualitative than quantitative. However, it can be seen that both codes largely under predict the creep rate and strain at the experimental failure time, and that for some of experiments there are substantial differences. This observation can be easily verified if we take a closer look at any specific experiment simulation case. Timely change of pressure tube average circumferential strain for experiment F-286 is given in Figures 4 and 5, as an example. Figure 4 shows comparison of PTDFORM predictions for right and left halves of a pressure tube against experimental data. Similarly, Figure 5 shows comparisons of predictions by PTSTRAIN code against the same experimental data. In this figure we included also curves showing maximum local strain in addition to the averaged value for a whole tube. It is obvious that codes are under predicting data on average strain. It is quite interesting to note that curves showing maximum local strain (taken for a segment of pressure tube with fastest straining) are much closer, but still under predicting experimental data. The same trend is observed in other experiment's simulation cases.

**Figure 4**  
**Comparison of PTDFORM Predictions of Tube Average Strain for Experiment F-286**



Further, if one recalls that experiments showed also longitudinal strain to a certain extent (locally, in the order of 10-30%, except for experiments E and H) we may come to the conclusion that overall simulation results are not very much in favour of validity of the computer codes used to assess the pressure tube ballooning. Limited parametric tests performed with the AECBALL code, allowing some longitudinal straining and departure from cylindrical geometry of the tube improved the simulation results pushing them toward the values of diametral strain at failure as observed in the experiments. But since these effects were encountered purely, arbitrarily, great care should be taken in interpreting the results to avoid possible misleading conclusions. Another factor that may be contributing significantly to the poor agreement between the codes is clearly nonlinear character of the straining. One of the sources of nonlinearity may certainly be attributed to the localized irreversible heat generation due to the deformation work done on the pressure tube, particularly around the location of the failure. This effect is not considered in either one of the codes used for pressure tube integrity analysis. Obviously, ballooning and straining in the plastic deformation region cannot be easily addressed with the simple mechanistic models used in these codes.

**Figure 5**  
**Comparison of PTSTRAIN Predictions of Tube Average Strain for Experiment F-286**



Quite different behaviour was noticed in low pressure experiments with the slow temperature ramps of  $1 \text{ K s}^{-1}$ . As it can be seen from Figures 6 and 7, for the condition of experiments E and H, the codes' predictions are becoming much closer to the experimental data toward the termination of experiments. In these experiments, the pressure tube did not rupture since experiments were terminated when average strain passed 30%. This behaviour is expected since under these conditions the shape of the specimen changed toward the sphere around the mid plane. As the specimen becomes more spherical there is relaxation of the stress and tube tends to strain slower. This trend can be seen particularly on Figure 6, when there is a noticeable change in the slope of the strain measured at -30 mm location, from the mid plane. This phenomena may not have much of practical importance for ballooning in reactor conditions but must be taken into account in interpreting the results of these experiments.

**Figure 6**  
**Comparison between PTSTRAIN Predictions and Experimental Data**  
**for the Conditions of a Slow Temperature Ramp Experiment E-292**

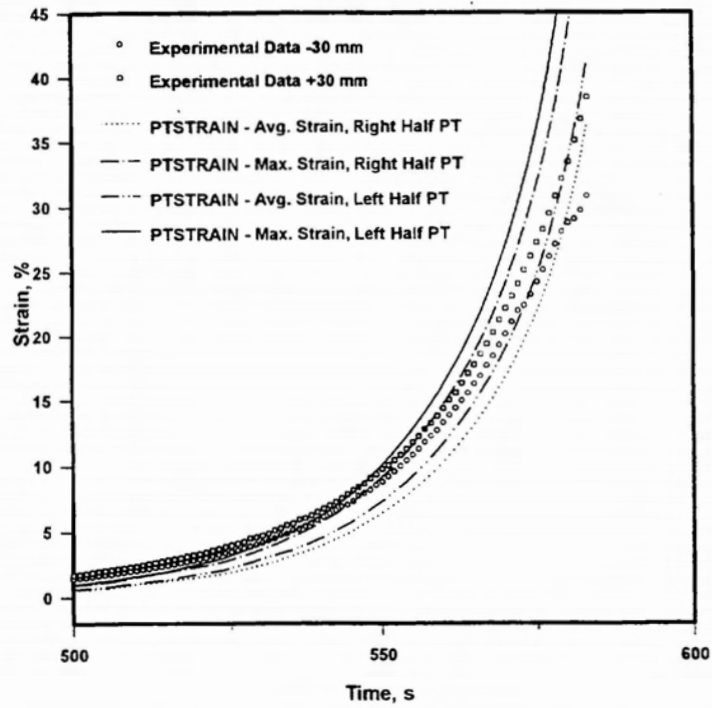


**Figure 7**  
**Comparison between PTDFORM Predictions and Experimental Data**  
**for the Slow Temperature Ramp Experiment H-304**

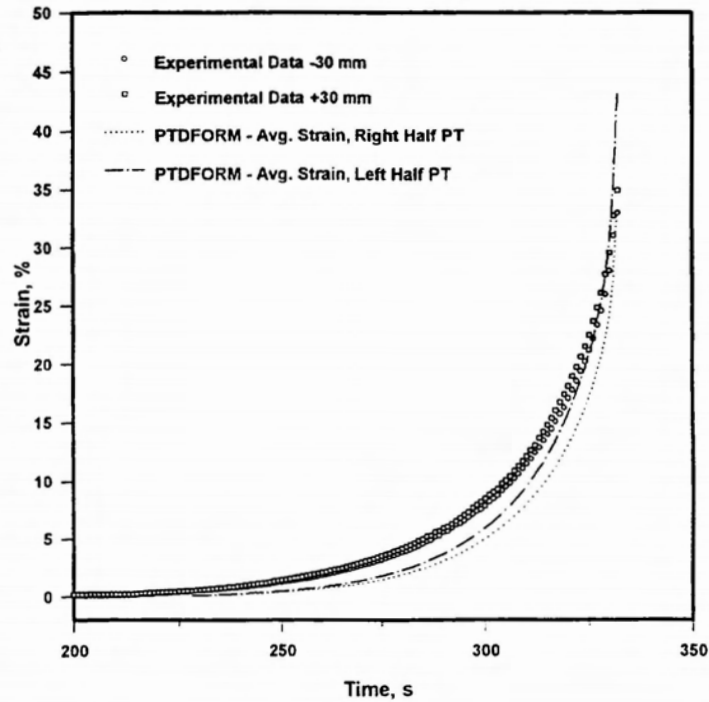
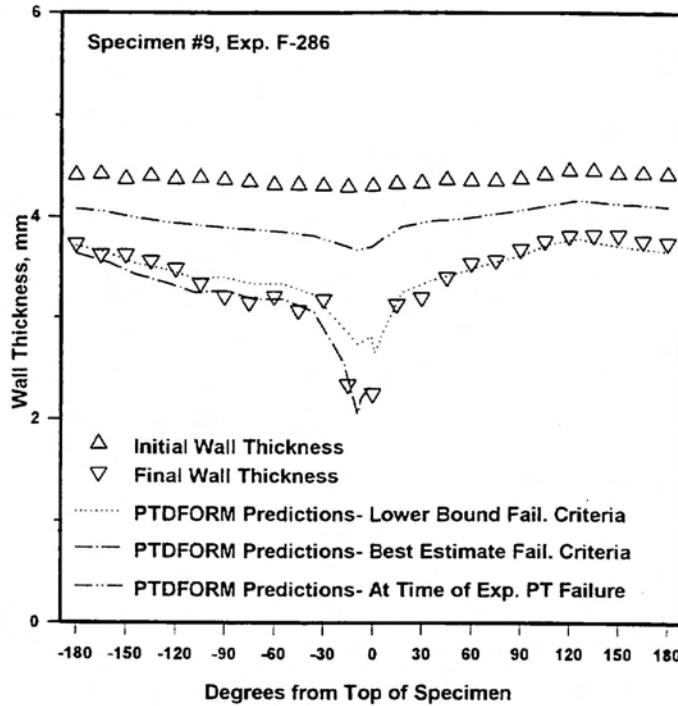


Figure 8 shows the change in wall thickness of the pressure tube specimen #9 which is used in experiment F-286. Final wall thickness measurements were done after experiment on a ruptured tube. In this figure we also showed predictions of circumferential wall thickness variation as predicted by PTDFORM. One can see that for this particular case, code predictions agree reasonably well with experimental data. Also, it can be seen that wall thickness values further from the location of rupture follow more closely code results as taken at the time interval when a lower bound failure criterion was met. In the region around the rupture, code predictions based on the best estimate failure criteria are much closer to experimentally observed wall thicknesses than those of lower bound criteria.

**Figure 8**  
**Wall Thickness Change for Specimen in Experiment F-286**



## CONCLUSIONS

Three computer codes, PTDFORM, PTSTRAIN and AECBALL, were used to simulate the newly performed Phase 5 experiments of an AECB experimental program on pressure tube ballooning. The overall agreement of the codes' predictions was rather qualitative than quantitative. While times to rupture were predicted with reasonable accuracy, it was found that codes largely under predict pressure tube staining. Phenomenology of the tube straining and failure mechanism and their mathematical description in the models built in these computer codes is out of the scope of this exercise, but it is certainly a key factor which influences the quality of predictions and their interpolation to the pressure tube ballooning under real, in-reactor conditions. Hydrogen blisters did not seem to affect the circumference at rupture even though they cracked and greater strain was observed around the blisters. Because of this and since the pressure tube which was ballooned in hydrogen picked up all the hydrogen in it, it may be useful to balloon a tube with a larger source of hydrogen to see if creep is affected by high bulk hydrogen content.

## Acknowledgement

The authors would like to express their sincere appreciation to the Ontario Hydro and AECL staff for help in running the codes, and to Mr. Fraser Forrest for help in interpreting the experimental data. Particular thanks is to Mr. T. Byrne of OH Technologies for his calculations of the blister dissolution. We are grateful to R. Clark of AECB CQAD for

providing us with results of ANSYS/FLOTRAN analysis and to A. Shalabi for discussion of the pressure tube ballooning problem.

## REFERENCES

- (1) FORREST, C.F., "Ballooning of CANDU Pressure Tubes - Experiments with Degraded Tube Material," AECB Project No. 2.184.4, AECB Report, INFO-0556, 1995, June.
- (2) FORREST, C.F., "Ballooning of CANDU Pressure Tubes - Hydride Blisters and Iodine," AECB Project No. 2.184.5, Stern Laboratories Report, SL-095, 1997, April.
- (3) SHEWFELT, R.S.W., LYALL, L.W., GODIN, D.P., "A High-Temperature Creep Model for Zr-2.5 wt% Nb Pressure Tubes," Journal of Nuclear Materials, Vol. 125, pp. 228-235, 1984.
- (4) SHEWFELT, R.S.W., GODIN, D.P., LYALL, L.W., "Verification Tests of a High-Temperature Transverse Creep Model for Zr-2.5 wt% Nb Pressure Tubes," AECL Report AECL-7813, 1984.
- (5) ABOUD, R., "Description and Validation of PTDFORM Version 2.0," AECL CANDU Report TTR-424, 1992, August.
- (6) ABOUD, R., "Source Listing of PTDFORM Version 2.0," AECL CANDU Report TTR-425, 1992, August.
- (7) MUIR, W.C., BAYOUMI, M.H., "Prediction of Pressure Tube Ballooning under Non-Uniform Circumferential Temperature Gradients and High Internal Pressure," Proceedings of the Fifth International Conference on Simulation Methods in Nuclear Engineering, Montreal, September 8-11, 1996, Vol. 2.
- (8) KUNDURPI, P.S., "Validation of Computer Code NUBALL for Simulation of Pressure Tube Ballooning Behaviour," Proceedings of the Second International Conference on Simulation Methods in Nuclear Engineering, Montreal, 1986, October.
- (9) LOCKE, K.E., "SMARTT: A Computer Code to Predict Transient Fuel and Pressure Tube Temperature Gradients under Asymmetric Coolant Conditions," Ontario Hydro, Nuclear Studies & Safety Department Report No. 86007, 1987, March.
- (10) OLIVA, A.F., to EL-HAWARY, M.A., "Transfer of PTSTRAIN Version 1.1 code," Ontario Hydro, November 3, 1996.
- (11) CAMPBELL, M.R., "Computer Modelling of Pressure Tube Ballooning Behaviour," AECB Assessment Report 94-PRC-103 Addendum I, File 26-1-13-6-0, August 09, 1994.
- (12) GRANT, I.M., SHALABI, A.F., "Pressure Tube Ballooning in CANDU Reactors," AECB CQAD Assessment Report 95-PRC-106, September 06, 1995.
- (13) SHEWFELT, R.S.W., "Ballooning of CANDU Pressure Tubes - Model Assessment," AECB Research Report INFO-0551, 1990, February.
- (14) HOFMAN, P., "Determination of the Critical Iodine Concentration for Stress Corrosion Cracking Failure of Zircaloy-4 Tubes Between 500 and 900°C," Journal of Nuclear Materials, Vol. 107, pp. 297-310, 1982.
- (15) DAKIN, J.S., "Iodine Stress Corrosion Cracking Studies in Irradiated Zircaloy Cladding," Proceedings of the International Topical Meeting on Light Water Reactor Fuel Performances, West Palm Beach, Florida, pp. 601-608, April 17-21, 1994.
- (16) CLARK, R., "Flotran Analysis of Stern Pressure Tube Ballooning Tests," AECB Report 96-PRC-118, September 25, 1996.
- (17) DE CARUFEL, G., "Pressure Tube Ballooning Experiments Analysis," AECB Memorandum, 34-2-184-4, SED R-169, March 02, 1995.
- (18) RIZNIC, J., "Pressure Tube Ballooning Experiments Analysis," AECB Memorandum, 26-6-10479-0, 34-2-184-4&5, SED R-169, October 08, 1996.
- (19) RIZNIC, J., "Pressure Tube Ballooning Experiments Analysis - Attachment I," AECB Memorandum, 26-6-10479-0, 34-2-184-4&5, SED R-169, February 18, 1997.
- (20) SHOTKIN, L.M., "How the Code Analyst can Influence the Calculation and Use Good Practices to Minimize Pitfalls," Nuclear Technology, Vol. 117, (1), pp. 40-48, 1997.
- (21) HO, E.T.C., DONNER, A., "Characterization of Ballooned Zr-2.5 Nb Pressure Tubes," Ontario Hydro Technologies Report No. A-NFC-96-193-P, December 23, 1996.
- (22) BYRNE, T.P., "Computer Simulations for High Temperature Blister Dissolution," OH Technologies Report N-FC-5-5368-003-1995, Revision 1, January 31, 1996.